Journal of Organometallic Chemistry 695 (2010) 67–73

Contents lists available at ScienceDirect

Journal of Organometallic Chemistry

journal homepage: www.elsevier.com/locate/jorganchem

Multi-site coordination of ferrocenylamido-naphthyridine conjugates [{(5,7-dimethyl-1,8-naphthyridin-2-yl)amino}carbonyl]ferrocene and 1,1′-bis[{(5,7-dimethyl-1,8-naphthyridin-2-yl)amino}carbonyl]ferrocene

Nabanita Sadhukhan, Arup Sinha, Raj K. Das, Jitendra K. Bera *

Department of Chemistry, Indian Institute of Technology Kanpur, Kanpur 208 016, India

ARTICLE INFO

Article history:
Received 10 June 2009
Received in revised form 17 September 2009
Accepted 22 September 2009
Available online 29 September 2009

Keywords:
Ferrocene
Naphthyridine
Metallamacrocycle
Rhenium
Potassium encapsulation

ABSTRACT

Ferrocenylamido-naphthyridine conjugates [{(5,7-dimethyl-1,8-naphthyridin-2-yl)amino}carbonyl]ferrocene (L^1) and 1,1′-bis[{(5,7-dimethyl-1,8-naphthyridin-2-yl)amino}carbonyl]ferrocene (L^2) have been synthesized. Reaction of L^1 with $[Cu(CH_3CN)_6][ClO_4]_2$ affords $[Cu(L^1)_2][ClO_4]_2$ (**1**) demonstrating tridentate coordination of the ligand utilizing naphthyridine (NP) nitrogens and carbonyl oxygen. Hydroxo-bridged neutral dirhenium(I) compound $[K\subset\{\{Re(CO)_3\}_2(\mu\text{-}OH)(Fc(CONHNP)(CO\overline{N}\ NP))_2\}]$ (**2**) is reported in which the amido-NP arm of L^2 chelates a Re^I, and a K^+ ion is encapsulated in a six-coordinate environment rendered by four NP nitrogens and two carbonyl oxygens involving all four arms of two L^2 ligands. Selective and reversible binding of K^+ ion by the organometallic host has been recognized from electrochemical and fluorescence experiments. Partial hydrolysis of L^2 has provided a neutral metallamacrocycle $[\{Re(CO)_3\}_2\{Fc(CO_2)(CONHNP)\}_2]$ (**3**) consisting of alternate Fc and $Re(CO)_3$ units linked by carboxylate and amide-NP bridges. The rotational freedom of the ferrocenyl rings, the flexibility of the amide linker and the multi-site coordination of the ligands are demonstrated in the molecular structures of compounds **1**–**3**.

1. Introduction

Ditopic ligands incorporating flexible spacers are attractive candidates for making inorganic architectures [1]. The ferrocenyl spacers have been widely employed to introduce structural flexibility and organometallic functionality [2]. Two cyclopentadienyl (Cp) rotors induce conformational regulation in the flexible structures, and the electrochemical and optical characteristics of ferrocene unit justify their utility in the functional assemblies. Covalent attachment of donor units to ferrocene, linked directly or through molecular spacers, have resulted numerous organometallic ligands [3]. Transition metal compounds of these ligands have found broader applications in the field of catalysis [4], molecular sensor [5], non-linear optical materials [6], molecular magnets [7] and pharmaceuticals [8]. We have recently described the metal-driven self-assembly of naphthyridine–ferrocene–naphthyridine (NP–Fc–NP) hybrid ligand in the construction of mixed-metal assemblies including several novel metallamacrocycles [9].

Ferrocenylamide-containing molecules have played a central role in the development of molecular sensors [5]. Hydrogen-bonding interactions of the amide N–H hydrogens are directed towards molecular recognition of an anionic/neutral guest species [10]. Ferrocene unit is usually the probe, sensitive to small changes in electronic structure brought about by the substrate binding [11]. The amide twist is amply demonstrated in the self-assembled structure of ferrocenyl peptides aided by H-bonding interactions [12]. In continuation of our interest in the preparation of mixed-metal assemblies involving ferrocene derivatives [9], we have incorporated ferrocenylamide group to the naphthyridine unit. The mono and bis-substituted ferrocenylamido-naphthyridine conjugates, [{(5,7-dimethyl-1,8-naphthyridin-2-yl)amino}carbonyl]ferrocene (FcCONHNP = L^1) and 1,1′-bis[{(5,7-dimethyl-1,8-naphthyridin-2-yl)amino}carbonyl]ferrocene ($Fc(CONHNP)_2 = L^2$) (Scheme 1) are reported. In addition to N donors of the NP unit, the carbonyl oxygen and the amide nitrogen provide additional binding sites. Synthesis and coordination chemistry of organometallic ligands L^1 and L^2 with a selected set of transition metal ion/fragment is described herein.

2. Results and discussion

2.1. Ligands L^1 and L^2

Ferrocene based ligands L^1 and L^2 are synthesized by the general reaction of (5,7-dimethyl)-2-amino-1,8-naphthyridine and corresponding chlorocarbonyl-ferrocene at an appropriate ratio in presence of freshly distilled triethylamine. Both ligands are characterized by NMR and IR spectra. The amide protons at δ 9.39 and

* Corresponding author. Tel.: +91 512 259 7336; fax: +91 512 259 7436.
E-mail address: jbera@iitk.ac.in (J.K. Bera).

0022-328X/$ - see front matter © 2009 Elsevier B.V. All rights reserved.
doi:10.1016/j.jorganchem.2009.09.029

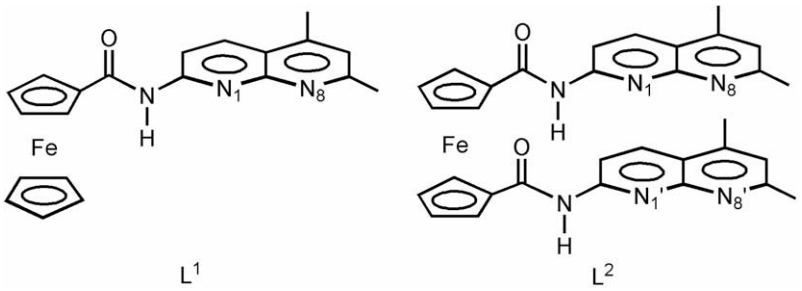

Scheme 1. Line drawings of L^1 and L^2.

8.5 ppm, strong carbonyl stretching frequencies at 1678 and 1672 cm^{-1}, and $[M+H]^+$ signals at *m/z* 386 and 585 in ESI-MS are characteristics for L^1 and L^2, respectively. Solid-state structures are confirmed from X-ray crystallography.

The asymmetric unit of L^1 consists of two crystallographically independent molecules along with two waters. Two near parallel Cp rings are eclipsed. The amide and the associated Cp ring are planar (vide infra) reflecting effective electron delocalization [13]. The disposition of the carbonyl O and N atoms of NP unit is anti to each other. Thus, it provides a DAA type H-bonding site involving amide N–H as donor and two N atoms of NP as acceptors. Crystal structure reveals that two molecules of L^1, facing each other, engage in H-bonding contacts with two lattice water molecules as shown in Fig. 1. The calculated (N)–H···O distances are 2.099 and 2.028 Å, and (O)–H···N distances are in the range 1.852–2.257 Å. The metrical parameters are similar for two L^1 molecules in the asymmetric unit with an important exception. The angle between the Cp and NP planes are different, and the values are 9.7° and 24.3°.

The essential structural features of L^2 are similar to L^1. The Cp and amide units are planar, and the carbonyl O and N atoms of NP are in opposite faces of the molecule. Interestingly, the Cp rings and the amide-NP arms are perfectly eclipsed. Syn-eclipsed configuration has been reported for a dimer adduct of bis-substituted metallocenylamido-pyridine molecules linked by glutaric acid [14]. Careful examination of the crystal structure of L^2 reveals a similar dimer formation involving four lattice water molecules (Fig. 2). Four water O atoms are coplanar affording single hydrogen-bond acceptor site for amide H and four hydrogen atoms, oriented above and below to the rectangle plane, further linked with NP N atoms by hydrogen-bond interactions. The water tetramer adopts a D_{2h} symmetry [15], and the calculated (O)–H···O and (N)–H···O distances are shown in Figure S7.

2.2. $[Cu(L^1)_2][ClO_4]_2$ (**1**)

Despite our earlier success in obtaining numerous mixed-metal compounds with Fc–NP hybrid ligands [9], complexation reactions of L^1 and L^2 and subsequent isolation of the coordination complexes turned out to be a challenging task. Reaction of L^1 with $[Cu(CH_3CN)_6][ClO_4]_2$ in acetonitrile affords $[Cu(L^1)_2][ClO_4]_2$ (**1**). The molecular structure of the dicationic unit $[Cu(L^1)_2]^{2+}$ in **1** is portrayed in Fig. 3 and selected metrical parameters are given in the corresponding figure caption. Two L^1 ligands coordinate to the central copper atom in *mer*-octahedral geometry. Each ligand chelates copper in a tridentate fashion involving NP N atoms and carbonyl O forming the meridional plane. The *cisoid* disposition

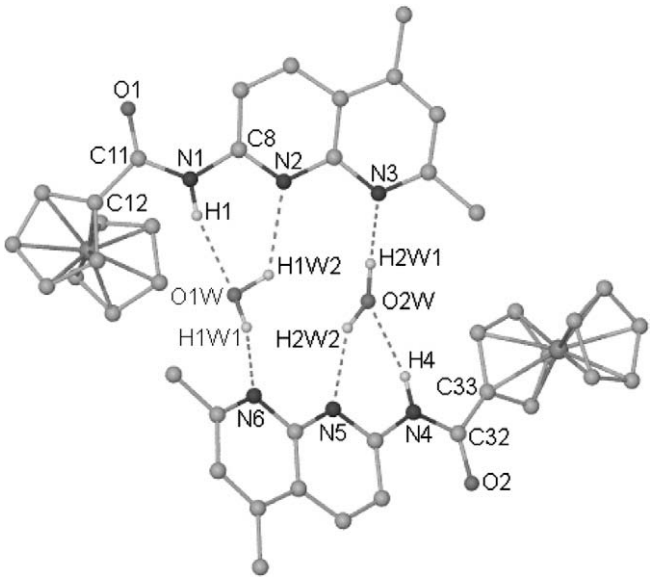

Fig. 1. Diagram of the L^1 dimer engaged via H-bonding interaction with two water molecules. All hydrogen atoms except amide and water H are omitted for the sake of clarity. Selected bond distances (Å) and angles (°) in an independent molecule: O1–C11 1.225(5), O1–C32 1.230(4), N1–H1···O1W 2.099, N4–H1···O2W 2.028, N2···H1W2–O1W 2.257, N3···H2W1–O2W 1.852, N5···H2W2–O2W 1.998, N6···H1W1–O1W 1.987, N1–C11–C12 114.4(3), C11–N1–C8 128.9(3), N4–C32–C33 114.4(3), C32–N4–C29 128.9(3).

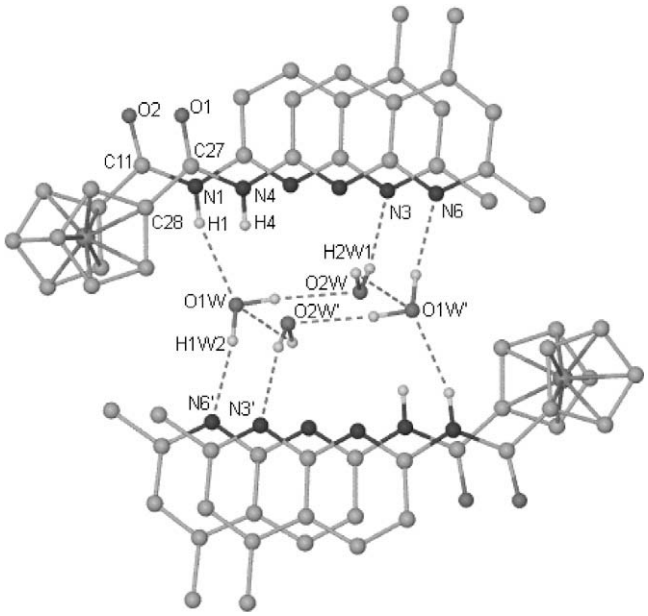

Fig. 2. Diagram of the L^2 dimer engaged via H-bonding interaction with four water molecules. All hydrogen atoms except amide and water H are omitted for the sake of clarity. Selected bond distances (Å) and angles (°): O1–C27 1.220(4), C11–O2 1.223(4), N1–H1···O1W 2.264, N4–H4···O2W′ 2.737, O1W–HIW2···N6′ 2.158, O2W–H2W1···N3 2.094, N4–C27–C28 116.4(3), O1–C27–C28 120.4(3), O1–C27–N4 123.1(3).

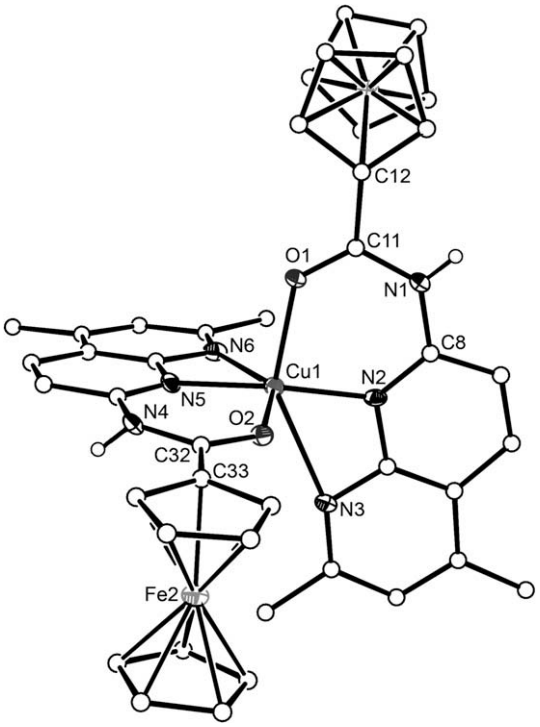

Fig. 3. ORTEP diagram (50% probability thermal ellipsoids) of $[Cu(L^1)_2]^{2+}$ in **1** with important atoms labeled. Carbon atoms are shown as circles of arbitrary radius. Hydrogen atoms except amide H are omitted for the sake of clarity. Selected bond distances (Å) and angles (°): Cu1–N5 1.918(3), Cu1–N2 1.924(3), Cu1–O1 2.049(3), Cu1–O2 2.075(3), Cu1–N3 2.512(4), Cu1–N6 2.533(3), N5–Cu1–N2 168.01(14), N5–Cu1–O1 100.56(12), N2–Cu1–O1 87.46(13), N5–Cu1–O2 86.78(12), N2–Cu1–O2 99.69(12), O1–Cu1–O2 105.86(11), N5–Cu1–N3 111.08(13), N2–Cu1–N3 59.37(13), O1–Cu1–N3 145.81(12), O2–Cu1–N3 88.97(11), N5–Cu1–N6 58.87(12), N2–Cu1–N6 113.24(12), O1–Cu1–N6 87.05(11), O2–Cu1–N6 145.24(11), N3–Cu1–N6 98.13(11).

of the coordinating atoms, accessed via rotation of the C–N bond, is in sharp contrast to their anti configuration in the free ligand. A drop in C–O stretching frequency ($\nu_{C=O}$ = 1643 cm^{-1}) in comparison to the free ligand indicates coordination of the carbonyl oxygen. The distal N atom (N_8) of NP makes longer Cu–N distance (Cu1–N3 2.512(4) Å and Cu1–N6 2.533(3) Å) compared to the proximal N atom (Cu1–N2 = 1.924(3) Å, Cu1–N5 = 1.918(3) Å). Short Cu–O distances (Cu1–O1 = 2.049(3) Å; Cu1–O2 = 2.075(3) Å) and N–Cu–O angles (N5–Cu1–O2 = 86.78(12); N2–Cu1–O1 = 87.46(13)°) indicate strong chelate formation with carbonyl O and proximal N of NP. The angles N3–Cu1–N2 59.37(13)°, N6–Cu1–N5 58.87(12)°, O1–Cu1–O2 105.86(11)° illustrate the distorted octahedron geometry of the copper atom.

The UV–Vis absorptions, emission wavelengths and electrochemical potentials for L^1, L^2 and compounds **1**–**3** are given in Table 1. The low-energy absorption of **1** is red shifted by 41 nm from the free ligand L^1. Cyclic voltammogram of **1** exhibits Fc/Fc^+ couple at 0.69 V, shifted 40 mV to higher potential from L^1.

2.3. [K{{Re(CO)$_3$}$_2$(μ-OH)(Fc(CONHNP)(CONNP))$_2$}] (**2**)

Deprotonation of L^2 by ^{t}BuOK and subsequent reaction with $Re(CO)_5Cl$ provided potassium-encapsulated hydroxo-bridged neutral dirhenium(I) compound [K⊂{{$Re(CO)_3$}$_2$(μ-OH)(Fc(CONHNP)(CONNP))$_2$}] (**2**) in high yield. The ORTEP diagram of **2** is shown in Fig. 4 and relevant metrical parameters are given in the corresponding figure caption. A crystallographically imposed C_2 symmetry results in half of the molecule in the asymmetric unit. Complex **2** consists of two [$Re^I(CO)_3$] fragments linked by single hydroxo bridge. Each Re atom is further coordinated to two N atoms from the deprotonated arm of L^2. The deprotonated amide N and the proximal N of NP chelate the rhenium atom (Re1–N6 = 2.219(5); Re1–N5 = 2.176(5) Å). Small N–Re–N angle of 59.44(17)° essentially imposes distorted octahedral geometry to the rhenium. Dirhenium(I) complexes bridged by a single hydroxy group are few reported in literature [16]. The Re···Re distance 3.9509(5) Å, Re–O(H) distance 2.138(2) Å and Re–O(H)–Re angle 135.1(3)° are similar to that reported for [{$Re(CO)_3(bipy)$}$_2$(μ-OH)][SbF_6] [17].

The most remarkable aspect of complex **2** is the encapsulation of K^+ ion inside the cavity rendered by amide-NP arms of two L^2 ligands. Each ligand provides three sites for K binding, two NP N atoms from one arm and the carbonyl O from the second arm. The angles formed by two cis coordinating atoms and potassium range from 48.38(14)° (N1–K1–N2) to 123.72(3)° (O2–K1–O2′). The K1–N1 and K1–N2 distances are 2.740(5) and 2.827(5) Å, respectively, and K1–O2 distance is 2.695(4) Å. The synclinal-eclipsed conformation of ferrocenyl rings is noticed in this complex with rotational angle 73.9° [9,18].

2.4. Selective and reversible binding of K^+ Ion

Cyclic voltammetry (CV) of **2** in acetonitrile reveals an irreversible Fc/Fc^+ couple at $E_{p,a}$ = 0.94 V. Addition of excess 18-crown-6 resulted in the shift of the potential to 1.15 V. The anodic shift of 210 mV is contrary to the expectation that removal of positively charge K^+ from the metallacage would make ferrocene oxidation easier [19]. We offer an explanation for the observed anodic shift upon decomplexation of K^+ from the organometallic host. The Fc/Fc^+ oxidation in free L^2 ligand occurs at $E_{p,a}$ = 0.82 V which is substantially higher towards positive potential compared to ferrocene ($E_{1/2}$ = 0.52 (70) V). This is attributed to the electron-withdrawing effect of amide-NP appendages in Cp rings. Solid-state structure of L^2 reveals near-planar arrangement of Cp and amide units indicating effective electron delocalization. The planarity is significantly lost when amide-NP arms are coordinated to metal ions as in **2**. Relevant dihedral angles illustrate this fact. The C_1(Cp)–C_2(Cp)–C(amide)–O(amide) angles (C_2 is the ipso carbon; C_1 is the adjoined carbon) in L_2 are 0.2°, 1.3°, 10.7° and 11.1°. The amide arm which is engaged in N–H···O interaction with lattice water (Fig. 2) exhibits higher torsional angles compared to the free amide. The corresponding angles in compound **2** are 18.1°, 20.2°, 31.8° and 35.8°. The amide oxygens which are coordinated to K^+ result in higher dihedral angles. It is our contention that removal of K^+ leads to reinstatement of planar arrangement between Cp and amide units allowing charge depletion from the Cp ring. This makes the ferrocene oxidation difficult upon removal of the K^+ ion.

Consequently, CV titration of **2** was performed against 18-crown-6. On sequential addition of 18-crown-6 to the acetonitrile solution of **2**, an anodic drift at $E_{p,a}$ = 1.15 V emerges passing through an isopotential point at 1.033 V (Fig. 5). CV experiences no further change upon addition of 1.1 equivalents of 18-crown-6 suggesting complete exchange of K^+ ion.

Reversibility and selectivity of potassium binding process in **2** was investigated by UV–Vis absorption and emission spectroscopy. The electronic spectra of **2** shows absorption at λ_{max} = 241 and 331 nm whereas a broad emission spectrum was recorded ranging from 330 to 470 nm upon excitation at λ_{ex} = 320 nm. Addition of 18-crown-6 to **2** brought about no appreciable change in the optical spectra. However, a fivefold enhancement of emission intensity at 388 nm was observed on addition of excess 18-crown-6. Fluorescence titration revealed a ratiometric response with gradual addition of 18-crown-6 (Fig. 6). The stepwise increase of fluorescent intensity reaches at maxima upon addition of 1.1 equiv of 18-crown-6 and further addition does not show any effect to the

Table 1
Electronic absorption and emission spectral data in acetonitrile and cyclic voltammetric[d] data (in volt) for L^1, L^2 and compounds **1**–**3** at room temperature.

Compounds	Absorption spectra			Emission spectra		Cyclic voltammogram	
	λ_{max}, nm (log ε)			Excitation (nm)	λ_{max} emission (nm)	λ_{max} Fc-center	NP-center
L^1	238 (3.88)	331 (3.58)	451 (3.24)	350	397	0.65 (100)[a]	−1.84[c]
L^2	238 (4.77)	334 (4.62)	461 (4.02)	320	396	0.82[b]	−1.98[c]
1	236 (4.37)	335 (3.96)	492(2.99)	260	380	0.69 (130)[a]	−1.79[c]
2	241 (4.80)	329 (4.50)	386 (4.07)	320	388	0.94[b]	−1.93[c]
3	238 (4.58)	331 (4.27)	451 (3.16)	331	405	0.97[b], 0.81[c]	−1.80[c]

[a] Half-wave potentials evaluated from cyclic voltammetry as $E_{1/2} = (E_{p,a} + E_{p,c})/2$, peak potential differences in mV in parentheses.
[b] Peak potentials, $E_{p,a}$ for irreversible processes.
[c] Peak potentials, $E_{p,c}$, for irreversible processes.
[d] Cyclic voltammetric studies were performed in acetonitrile for L^1, L^2, **2**; and in propylene carbonate for **1** and **3**.

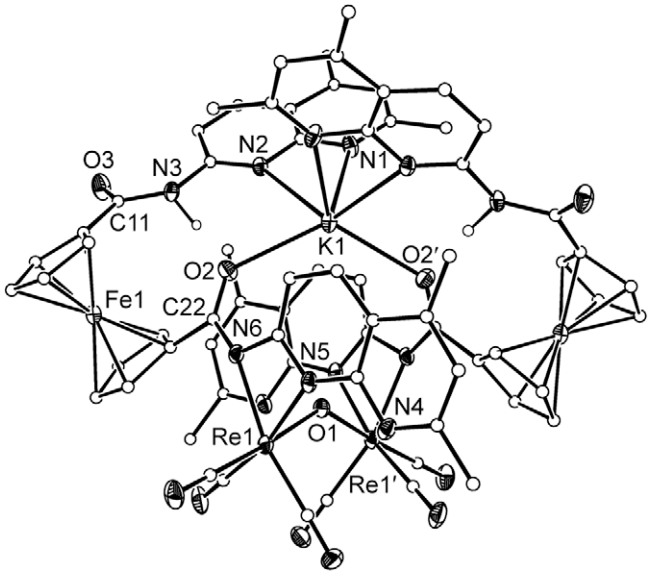

Fig. 4. ORTEP diagram (50% probability thermal ellipsoids) of [K⊂{{Re(CO)$_3$}$_2$(μ-OH)(Fc(CONHNP)(CONNp))$_2$}] (**2**) with important atoms labeled. Carbon atoms are shown as circles of arbitrary radius. Hydrogen atoms except amide H are omitted for the sake of clarity. Selected bond distances (Å) and angles (°): Re1–O1 2.138(2), Re1–N5 2.176(5), Re1–N6 2.219(5), N2–K1 2.827(5), O2–K1 2.695(4), N1–K1 2.740(5), Re1···Re1′ 3.9509(5), O1–Re1–N5 81.47(16), O1–Re1–N6 80.16(18), N5–Re1–N6 59.44(17), Re1′–O1–Re1 135.1(3), O2′–K1–O2 123.7(2), O2′–K1–N1 96.64(14), O2–K1–N1 123.01(13), O2′–K1–N2 134.22(13), O2–K1–N2 75.08(13), N1–K1–N2 48.38(14). Symmetry code: $-x, y, -z + 3/2$.

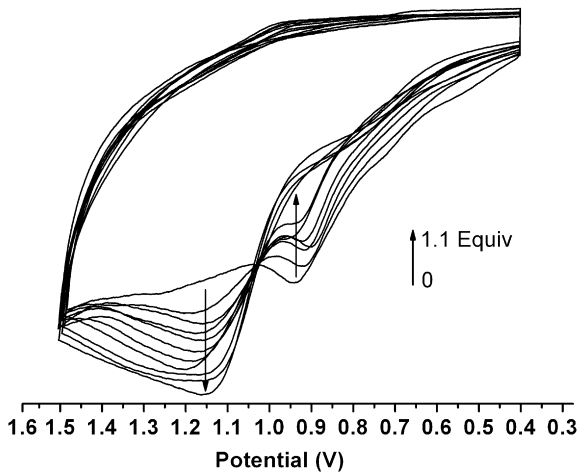

Fig. 5. Electrochemical potential change in cyclic voltammogram (Fc/Fc$^+$ couple) for **2** in acetonitrile with the gradual addition of 18-crown-6 (0–1.1 equiv).

fluorescence intensity (see inset in Fig. 6). It is established from the fluorescence and electrochemical experiments that complete release of K^+ from organometallic host **2** is achieved when 1.1 equivalents of 18-crown-6 is added.

Subsequent addition of K^+ to this solution resulted in a decrease in fluorescence intensity reaching to a value similar to that of **2** when excess K^+ is added. Addition of a range of monovalent cations such as Na^+, Cu^+, Tl^+, Ag^+, NH_4^+, and Hg^+ to the acetonitrile solution of 1:1 mixture of **2** and 18-crown-6 display marginal decrease in the fluorescence intensity (see Fig. S6) confirming selective K^+ binding over other metal ions.

It is therefore concluded that the exchange of K^+ ion from compound **2** to 18-crown-6 proceeds with concomitant structural change in the organometallic host which is reflected in the fluorescence enhancement. The original ligand conformation of **2** is regained when K^+ ions are fed into the solution. Such structural recovery is not observed for other monovalent metal ions illustrating the reversible and selective binding of K^+ ion by the organometallic host.

In order to gain insight on the effect of K^+ decomplexation on the structure of **2**, NMR spectroscopic measurements were carried out. Complex **2** contains two sets of non-equivalent protons belonging to the amide-NP and amido-NP arms. However, ^{1}H NMR spectrum reveals four sets of NP protons of equal intensity

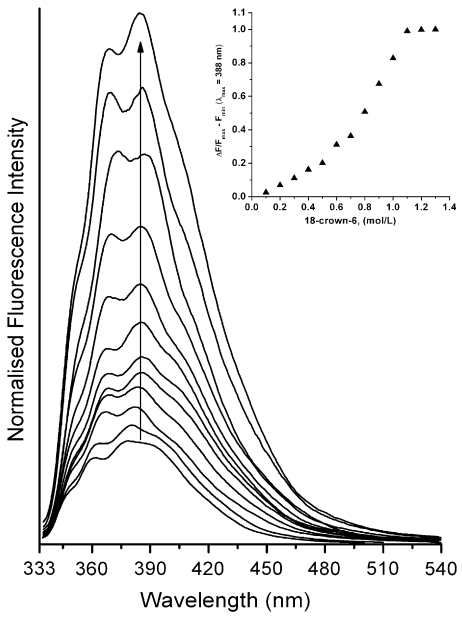

Fig. 6. Emission spectral change (λ_{ex} = 320 nm) for **2** (1.6×10^{-5} M) in acetonitrile with the gradual addition of 18-crown-6 (0–1.3 equiv). The corresponding normalized intensity enhancement monitored at 388 nm is presented in inset.

in the aromatic region, each set constituting three independent protons (Fig. S11). Each ligand possesses an element of planar chirality induced by metal coordinations, and two ligands have opposite chirality related by a center of inversion. The appearance of four sets of NP protons reflects two diastereoisomers present in solution. Addition of 18-crown-6 (two equivalents) to a CD_2Cl_2 solution of **2** and immediate recording of the ^1H NMR spectrum reveals complex spectrum with numerous signals in the aromatic region. This implies a mixture of **2** and its K^+ free congener. However, recording of the spectrum after 4 h at room temperature unveils only one set of NP protons. The decomplexation of K^+ from **2** leads to disengagement of the amide-NP arms of L^2. It is proposed that, upon removal of K^+, the amide and amido N atoms of each ligand chelate one rhenium forming a symmetric structure. A rapid hydrogen exchange between the coordinated nitrogens in the NMR time scale results in a single set of NP protons.

IR spectra of **2** did not reveal any significant changes upon treatment with 18-crown-6. The carbonyls frequencies of the 'Re(CO)$_3$' core are shifted marginally (2021 and 1894 cm^{-1}), but the amido-carbonyl absorptions are masked by the naphthyridine absorptions.

2.5. [{Re(CO)$_3$}$_2${Fc(CO$_2$)(CONHNP)}$_2$] (**3**)

The treatment of L^2 with NaH and subsequent treatment with $Re(CO)_5Cl$ resulted in the neutral metallamacrocycle [{Re(CO)$_3$}$_2$-{Fc(CO$_2$)(CONHNP)}$_2$] (**3**). Poor solubility of the compound in common organic solvents hindered its full characterization. However, the molecular structure was determined by X-ray study (Fig. 7). It reveals hydrolysis of one of the amide-NP arms to the corresponding carboxylate forming a molecular rectangle consisting of alternate Fc and $Re(CO)_3$ corners. Each $Re(CO)_3$ unit is coordinated to O atom of the carboxylate group in monodentate fashion, and N atoms of the NP from the second ligand chelate the metal ion. The Re2–O1 and Re1–O4 distances are 2.126(4), 2.156(4) Å, respectively, and the Re–N distances are in the range of 2.203(5)–2.234(5) Å. Small NP chelate angles N1–Re1–N2 59.52(16)° and N4–Re2–N5 60.16(17)° provide distorted octahedral geometry of rhenium with facial arrangement of three carbonyl ligands. The anticlinal-eclipsed arrangements of the two Cp rings having rotational angle 126.3° is the prerequisite for such a rectangular shaped metallacycle.

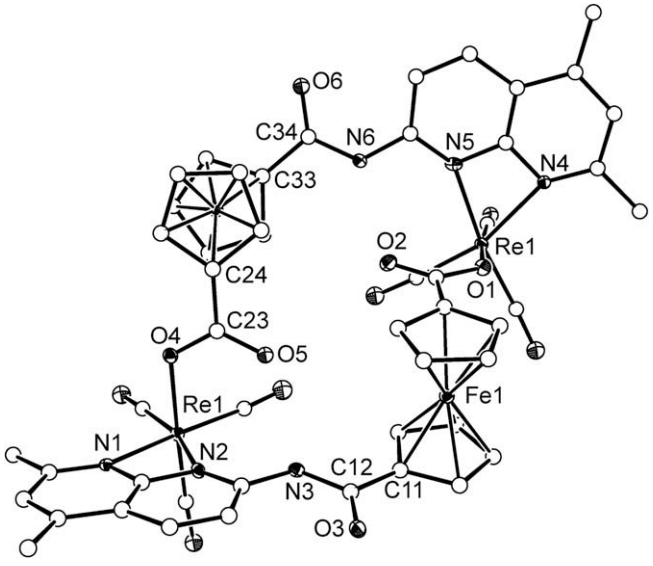

Fig. 7. ORTEP diagram (50% probability thermal ellipsoids) of [{Re(CO)$_3$}{Fc(CO$_2$)(CONHNP)}]$_2$ (**3**) with important atoms labeled. Carbon atoms are shown as circles of arbitrary radius. Hydrogen atoms except amide H are omitted for the sake of clarity. Selected bond distances (Å) and angles (°): Re1–O4 2.156(4), Re1–N2 2.227(5), Re1–N1 2.228(4), Re2–O1 2.126(4), Re2–N5 2.203(5), Re2–N4 2.233(4), O4–Re1–N2 81.73(16), O4–Re1–N1 83.74(15), N2–Re1–N1 59.52(16), O1–Re2–N5 82.61(16), O1–Re2–N4 82.26(15), N5–Re2–N4 60.16(17).

3. Summary

Incorporation of one and two amide-NP arms to ferrocene afforded organometallic ligand L^1 and L^2, respectively. The rotational flexibility of the ferrocenyl rings, the plasticity of the amide linker and different modes of the NP coordination to the metal afforded new mixed-metal compounds. Tridentate coordination of L^1 is confirmed in the Cu^{II} complex **1** utilizing NP nitrogens and carbonyl oxygen. In complex **2**, the amido-NP arm of L^2 chelates a Re^I, and a K^+ ion is encapsulated in a six-coordinate environment rendered by all four arms of two L^2 ligands. Selective and reversible binding of K^+ ion by the organometallic host {Re(CO)$_3$}$_2$(μ-OH)(Fc(CONHNP)(CONNP))$_2$} has been examined. Partial hydrolysis of L_2 provides a ligand which forms a neutral metallamacrocycle involving two 'Re(CO)$_3$' cores linked by two Fc(CO$_2$)(CONHNP) units. Multiple binding sites and the flexibility of these ligands make them prospectus candidates to develop mixed-metal assemblies for various applications.

4. Experimental

4.1. General procedures, materials and physical measurements

All reactions were carried out in air unless otherwise mentioned. Solvents were purified by conventional methods. The $Re(CO)_5Cl$, ^{t}BuOK, NaH and ferrocene were purchased from Aldrich. Compounds $[Cu(CH_3CN)_6][ClO_4]_2$ [20], chlorocarbonyl-ferrocene [21], 1,1′-bis(chlorocarbonyl)ferrocene [22], and 2-amino-5,7-dimethyl-1,8-naphthyridine [23] were prepared by following literature procedures. Elemental analyses were carried out on a Thermoquest CE instruments model EA/110 CHNS-O elemental analyzer. Samples were powdered and dried in vacuum for a prolonged period (8–16 h) prior to elemental analyses which gave consistent values. ESI-MS were recorded on a Waters Micromass Quattro Micro triple-quadrupole mass spectrometer. ^1H NMR was obtained on a JEOL JNM-LA 400 MHz spectrophotometer. Infrared spectra were recorded on a Bruker Vertex 70 FTIR spectrophotometer in the ranges from 400 to 4000 cm^{-1} using KBr pallets. Electronic absorptions were measured on Perkin–Elmer Lambda-20 UV–Vis spectrophotometer. Cyclic voltammetric studies were performed on a BAS Epsilon electrochemical workstation in acetonitrile with 0.1 M tetra-*n*-butylammonium hexafluorophosphate ($TBAPF_6$) as the supporting electrolyte. The working electrode was a BAS Pt disk electrode, the reference electrode was Ag/AgCl and the auxiliary electrode was a Pt wire. The scan rate is 100 mVs^{-1}. The $E_{1/2}$ is described by $(E_{p,a} + E_{p,c})/2$ reported in volts (V), and the value in parenthesis is ΔE ($E_{p,a} - E_{p,c}$) reported in millivolts (mV). The ferrocene/ferrocenium couple occurs at $E_{1/2}$ = +0.51 (70) V versus Ag/AgCl under the same experimental conditions.

4.2. Syntheses

4.2.1. Synthesis of L^1

Freshly prepared (chlorocarbonyl)ferrocene (500 mg, 2.0 mmol) in anhydrous tetrahydrofuran (30 mL) was added dropwise to the stirring mixture of triethylamine (290 mg, 2.85 mmol) and 2-amino-5,7-dimethyl-1,8-naphthyridine (400 mg, 2.30 mmol) in anhydrous tetrahydrofuran at 0 °C over a period of 30 min. The

reaction mixture was allowed to attain room temperature and stirred for additional 24 h. Solvent was removed under reduced pressure to afford an orange–red solid, which was purified by column chromatography on silica (ethyl acetate/petroleum ether; 9:1). Yield: 550 mg (70%). Single crystals were grown by the vapor diffusion of petroleum ether onto a dichloromethane solution of L^1. Anal. Calc. for $FeC_{21}H_{19}N_3O$: C, 65.47; H, 4.97; N, 10.91. Found: C, 65.42; H, 4.85; N, 10.87%. ESI-MS: *m/z* 386 $[M+H]^+$. IR (KBr, cm^{-1}): 3450 (s), 1678 (s), 1601 (s), 1511 (s), 1404 (m), 1314 (s), 1285 (s), 1138 (m), 854(m). ^1H NMR ($CDCl_3$, δ): 9.39 (br, 1H, NH), 8.68 (s, 1H, NP), 8.37 (s, 1H, NP), 7.19 (s, 1H, NP), 4.97 (s, 2H, Cp), 4.52 (s, 2H, Cp), 4.27 (s, 5H, Cp), 2.82 (s, 3H, CH_3), 2.71 (s, 3H, CH_3).

4.2.2. Synthesis of L^2

1,1′-Bis(chlorocarbonyl)ferrocene (750 mg, 2.40 mmol) in anhydrous dichloromethane (30 mL) was added dropwise to a stirring mixture of triethylamine (550 mg, 5.42 mmol) and 2-amino-5,7-dimethyl-1,8-naphthyridine (875 mg, 5.00 mmol) in anhydrous dichloromethane (30 mL) at 0 °C over a period of 30 min. The reaction mixture was allowed to attain room temperature and stirred for additional 24 h. Solvent was removed under reduced pressure to afford an orange solid, which was purified by column chromatography on neutral alumina (methanol/CH_2Cl_2; 3:97). Yield: 1.10 g (76%). Single crystals were grown by the vapor diffusion of diethyl ether onto a methanol solution of L^2. Anal. Calc. for $FeC_{32}H_{28}N_6O_2$: C, 65.76; H, 4.83; N, 14.38. Found: C, 65.69; H, 4.92; N, 14.35%. ESI-MS: *m/z* 585 $[M+H]^+$. IR (KBr, cm^{-1}): 3411 (s), 1672 (s), 1603 (s), 1512 (s), 1437 (m), 1313 (s), 1285 (m), 1139 (m). ^1H NMR ($CDCl_3$, δ): 8.5 (br, 1H, NH), 8.42 (dd, 2H, NP), 8.07 (dd, 2H, NP), 6.97 (s, 2H, NP), 4.88 (s, 4H, Cp), 4.52 (s, 4H, Cp), 2.62 (s, 6H, CH_3), 2.49 (s, 6H, CH_3).

*4.2.3. Synthesis of $[Cu(L^1)_2][ClO_4]_2$ (**1**)*

L^1 (77 mg, 0.20 mmol) was added to an acetonitrile solution (20 mL) of $Cu(ClO_4)_2$ (25 mg, 0.09 mmol), and the mixture was stirred for 8 h at room temperature. Solution was concentrated, and 15 mL diethyl ether was added with stirring to induce precipitation. The resulting red solid residue was washed with diethyl ether (3 × 10 mL), and dried in a vacuum to afford **1**. Yield: 73 mg (75%). X-ray quality crystals were grown by layering petroleum ether onto a saturated dichloromethane solution of **1** inside an 8 mm o.d. vacuum-sealed glass tube. Anal. Calc. for $C_{42}H_{38}Cl_2Cu_1Fe_2N_6O_{10}$: C, 48.84; H, 3.71; N, 8.14. Found: C, 48.77; H, 3.69; N, 8.04%. IR (KBr, cm^{-1}): 2925 (s), 1643 (s), 1610 (m), 1503 (m), 1418 (m), 1290 (m), 1250 (m), 1224 (m), 1113(vs).

*4.2.4. Synthesis of $[K\{\{Re(CO)_3\}_2(\mu\text{-}OH)(Fc(CONHNP)(CO\overline{N}NP))_2\}]$ (**2**)*

A sample of L^2 (45 mg, 0.077 mmol) dissolved in 15 mL THF was treated with ice cooled THF solution of ^{t}BuOK (17 mg, 0.15 mmol). After 30 min of stirring, 25 mg (0.07 mmol) of $Re(CO)_5Cl$ was added at room temperature and refluxed for 12 h. Solution was concentrated and 15 mL of petroleum ether was added with stirring to induce precipitation. Orange solid residue was collected by filtration, washed with petroleum ether (3 × 10 mL) and dried in vacuum to afford **2**. Yield: 49 mg (79%). X-ray-quality crystals were grown by layering petroleum ether onto a dichloromethane solution of **2** inside an 8 mm o.d. vacuum-sealed glass tube. Anal. Calc. for $C_{70}H_{58}N_{12}O_{11}K_1Fe_2Re_2$: C, 47.70; H, 3.09; N, 9.54. Found: C, 47.57; H, 2.98; N, 9.61%. IR (KBr, cm^{-1}): 2924 (m), 2008 (s), 1872 (s), 1678 (m), 1600 (m), 1509 (m), 1454 (m), 1404 (m), 1350 (m), 1280 (m). ^1H NMR ($CDCl_3$,δ): 9.12 (br, 1H, NH), 8.84 (d, *J* = 10 Hz, 1H, NP), 8.62 (d, *J* = 10 Hz, 1H, NP), 8.44 (d, *J* = 10 Hz, 1H, NP), 8.26 (s, 1H, NP), 8.21 (d, *J* = 10 Hz, 1H, NP), 8.14 (d, *J* = 9 Hz, 1H, NP), 8.09 (d, *J* = 10 Hz, 1H, NP), 7.87 (d, *J* = 10 Hz, 1H, NP), 7.29 (m, 1H, NP), 7.12 (s, 1H, NP), 6.88 (s, 1H, NP), 6.63 (d, *J* = 10 Hz, 1H, NP), 5.11–5.02 (m, 10H, Cp), 4.74–4.67 (m, 6H, Cp), 2.72–2.51 (8s, 24H, Me).

*4.2.5. Synthesis of $[\{Re(CO)_3\}\{Fc(CO_2)(CONHNP)\}]_2$ (**3**)*

A sample of L^2 (50 mg, 0.080 mmol) was added to the ice cooled THF solution (15 mL) of NaH (4 mg, 0.017 mmol). After 30 min of stirring, 25 mg (0.07 mmol) of $Re(CO)_5Cl$ was added at room temperature and refluxed for 12 h. Solution was concentrated and 15 mL of petroleum ether was added with stirring to induce precipitation. Orange solid residue was collected by filtration, washed with petroleum ether (3 × 10 mL) and dried in vacuum to afford **3**. Yield: 35 mg (73%). X-ray-quality crystals were grown by layering petroleum ether onto a dichloromethane solution of **3** inside an 8 mm o.d. vacuum-sealed glass tube. Anal. Calc. for $C_{50}H_{36}N_6O_{12}Fe_2Re_2$: C, 42.99; H, 2.60; N, 6.02. Found: C, 42.89; H, 2.57; N, 6.11%. ESI: *m/z* 1397 (10%) $[M+H]^+$. IR (KBr, cm^{-1}): 2924 (m), 2854 (m), 2007 (s), 1881 (s), 1663 (s), 1600 (m), 1511 (m), 1461 (m), 1406 (m), 1344 (m), 1314 (m), 1248 (m), 1188 (m).

4.3. X-ray data collection and refinement

Detailed single-crystal X-ray data collection and refinement procedure are similar as reported earlier [1a]. The hydrogen atoms were included at geometrically calculated positions in the final stages of the refinement and were refined according to the 'riding model' unless mentioned otherwise. All non-hydrogen atoms were refined with anisotropic thermal parameters unless mentioned otherwise. Pertinent crystallographic data for compounds L^1, L^2 and **1**–**3** are summarized in Table S1.

Hydrogens for lattice water molecules and amide residue were located from difference Fourier map and refined with restraints. SQUEEZE option was applied in **2** to remove severely disordered solvent molecules which could not be modeled. The dichloromethane solvate molecule in **3** was found to be disordered and was modeled satisfactorily. Structure solution and refinement details are provided in the Supporting information.

Acknowledgements

JKB thanks the Department of Science and Technology (DST), India for financial support of this work through the Grant of Ramanna fellowship. NS, AS, and RKD thank the Council of Scientific and Industrial Research (CSIR), India for fellowship.

Appendix A. Supplementary data

CCDC 742052, 742053, 742054, 742055 and 742056 contains the supplementary crystallographic data for L^1, L^2 and **1**–**3**. These data can be obtained free of charge from The Cambridge Crystallographic Data Center via www.ccdc.cam.ac.uk/data_request/cif. Supplementary data associated with this article can be found, in the online version, at doi:10.1016/j.jorganchem.2009.09.029.

References

[1] (a) J.K. Bera, J. Bacsa, K.R. Dunbar, in: R.B. King (Ed.), Encyclopedia of Inorganic Chemistry, second ed., John Wiley & Sons, New York, 2005;
(b) S. Leininger, B. Olenyuk, P.J. Stang, Chem. Rev. 100 (2000) 853;
(c) M. Fujita, Chem. Soc. Rev. 27 (1998) 417;
(d) M. Fujita, M. Tominaga, A. Hori, B. Therrien, Acc. Chem. Res. 38 (2005) 369;
(e) M. Fujita, K. Ogura, Coord. Chem. Rev. 148 (1996) 249.
[2] (a) D.L. Reger, K.J. Brown, J.R. Gardinier, M.D. Smith, Organometallics 22 (2003) 4973;
(b) B. Neumann, U. Siemling, H.-G. Stammler, U. Vorfeld, J.G.P. Delis, P.W.N.M. van Leeuwen, K. Vrieze, J. Fraanje, K. Goubtiz, F.F. de Biani, P. Zanello, J. Chem. Soc., Dalton Trans. (1997) 4705.;
(c) D. Braga, M. Polito, M. Bracaccini, D. D'Addario, E. Tagliavini, D.M. Proserpio, F. Grepioni, Chem. Commun. (2002) 1080;
(d) D. Braga, M. Polito, D. D'Addario, E. Tagliavini, D.M. Proserpio, F. Grepioni, J.W. Steed, Organometallics 22 (2003) 1080;

(e) N. Das, A.M. Arif, P.J. Stang, M. Sieger, B. Sarkar, W. Kaim, J. Fiedler, Inorg. Chem. 44 (2005) 5798;
(f) F.A. Cotton, L.M. Daniels, C. Lin, C.A. Murillo, J. Am. Chem. Soc. 121 (1999) 4538.
[3] (a) D. Paolucci, M. Marcaccio, C. Bruno, D. Braga, M. Polito, F. Paolucci, F. Grepioni, Organometallics 24 (2005) 1198;
(b) U. Siemeling, U. Vorfeld, B. Neumann, H.-G. Stammler, Chem. Commun. (1997) 1723;
(c) A. Ion, J.-C. Moutet, E. Saint-Aman, G. Royal, S. Tingry, J. Pecaut, S. Menage, R. Ziessel, Inorg. Chem. 40 (2001) 3632;
(d) Y. Gao, B. Twamley, J.M. Shreeve, Organometallics 25 (2006) 3364;
(e) G. Li, Y. Song, H. Hou, L. Li, Y. Fan, Y. Zhu, X. Meng, L. Mi, Inorg. Chem. 42 (2003) 913.
[4] (a) C.K.A. Gregson, V.C. Gibson, J.N. Long, E.L. Marshall, P.J. Oxford, A.J.P. White, J. Am. Chem. Soc. 128 (2006) 7410;
(b) Z. Weng, S. Teo, T.S. Andy Hor, Organometallics 25 (2006) 4878;
(c) V.C. Gibson, N.J. Long, P.J. Oxford, A.J.P. White, D.J. Williams, Organometallics 25 (2006) 1932;
(d) R.C.J. Atkinson, K. Gerry, V.C. Gibson, N.J. Long, E.L. Marshall, L.J. West, Organometallics 26 (2007) 316;
(e) J. Eppinger, K.R. Nikolaides, M. Zhang-Presse, F.A. Riederer, G.W. Rabe, A.L. Rheingold, Organometallics 27 (2008) 736;
(f) W. Chen, W. Mbafor, M.S. Roberts, J. Whittall, J. Am. Chem. Soc. 128 (2006) 3922;
(g) C. Bolm, J. Rudolph, J. Am. Chem. Soc. 124 (2002) 14850;
(h) O.G. Mancheño, R.G. Arrayás, J.C. Carretero, J. Am. Chem. Soc. 126 (2004) 456;
(i) V.D.M. Hoang, P.A.N. Reddy, T.-J. Kim, Organometallics 27 (2008) 1026;
(j) Z. Weng, S. Teo, L.L. Koh, T.S.A. Hor, Organometallics 23 (2004) 3603.
[5] P.D. Beer, Chem. Commun. (1996) 689;
(b) F. Otón, A. Espinosa, A. Tárraga, P. Molina, Organometallics 26 (2007) 6234;
(c) J. Westwood, S.J. Coles, S.R. Collinson, G. Gasser, S.J. Green, M.B. Hursthouse, M.E. Light, J.H.R. Tucker, Organometallics 23 (2004) 946;
(d) A.S. Georgopoulou, D.M.P. Mingos, A.J.P. White, D.J. Williams, B.R. Horrocks, A. Houlton, J. Chem. Soc., Dalton Trans. (2000) 2969.
[6] (a) G. Li, Y.L. Song, H. Hou, L. Li, Y. Fan, Y. Zhu, X. Meng, L. Mi, Inorg. Chem. 42 (2003) 913;
(b) H.K. Sharma, K.H. Pannell, I. Ledoux, J. Zyss, A. Ceccanti, P. Zanello, Organometallics 19 (2000) 770;
(c) T. Farrell, T. Meyer-Friedrichsen, M. Malessa, D. Haase, W. Saak, I. Asselberghs, K. Wostyn, K. Clays, A. Persoons, J. Heck, A.R. Manning, J. Chem. Soc., Dalton Trans. (2001) 29;
(d) D.A. Davies, J. Silver, G. Cross, P.J. Thomas, J. Organomet. Chem. 631 (2001) 59.
[7] (a) J.S. Miller, A.J. Epstein, Angew. Chem., Int. Ed. Engl. 33 (1994) 385;
(b) B.D. Koivisto, S.A. Ichimura, R. McDonald, M.T. Lemaire, L.K. Thompson, R.G. Hicks, J. Am. Chem. Soc. 128 (2006) 690;
(c) G. Wang, C. Slebodnick, R.J. Butcher, M.C. Tam, T.D. Crawford, G.T. Yee, J. Am. Chem. Soc. 126 (2004) 16890;
(d) J.S. Miller, A.J. Epstein, W.M. Reiff, Chem. Rev. 88 (1988) 201;
(e) H. Hou, L. Li, Y. Zhu, Y. Fan, Y. Qiao, Inorg. Chem. 43 (2004) 4767;
(f) H. Hou, G. Li, L. Li, Y. Zhu, X. Meng, F. Yaoting, Inorg. Chem. 42 (2003) 428.
[8] (a) P. Kopf-Maier, H. Kopf, E.W. Neuse, Angew. Chem., Int. Ed. Engl. 23 (1984) 456;
(b) E. Hillard, A. Vessieres, L. Thouin, G. Jaouen, C. Amatore, Angew. Chem., Int. Ed. Engl. 45 (2006) 285;
(c) L.V. Popova, V.N. Babin, Y.A. Belousov, Y.S. Nekrasov, A.E. Snegireva, N.P. Borodina, G.M. Shaposhikova, O.B. Bychenko, P.M. Raevskii, N.B. Morozova, A.I. Liyina, K.G. Shitkov, Appl. Organomet. Chem. 7 (1993) 85;
(d) Z. Miklan, R. Szabo, V. Zsoldos-Mady, J. Remenyi, Z. Banoczi, Pep. Sci. 88 (2007) 108.
[9] (a) N. Sadhukhan, J.K. Bera, Inorg. Chem. 48 (2009) 978;
(b) N. Sadhukhan, S.K. Patra, K. Sana, J.K. Bera, Organometallics 25 (2006) 2914.
[10] (a) S.R. Collison, T. Gelbrich, M.B. Hursthouse, J.H.R. Tucker, Chem. Commun. 00 (2001) 555;
(b) J.E. Kingston, L. Ashford, P.D. Beer, M.G.B. Drew, J. Chem. Soc., Dalton Trans. 00 (1999) 251;
(c) C. Suksai, P. Leeladee, D. Jainuknan, T. Tuntulani, N. Muangsin, O. Chailapakul, P. Kongsaeree, C. Pakavatchai, Tet. Lett. 46 (2005) 2765.
[11] (a) H. Miyaji, S.R. Collinson, I. Prokeŝ, H.R. Tucker, Chem. Commun. (2003) 64;
(b) J.D. Carr, L. Lambert, D.E. Hibbs, M.B. Hursthouse, K.M.A. Malik, J.H.R. Tucker, Chem. Commun. (1997) 1649.
[12] (a) D.R. van Staveren, N. Metzler-Nolte, Chem. Rev. 104 (2004) 5931;
(b) T.-A. Okamura, K. Sakauye, N. Ueyama, A. Nakamura, Inorg. Chem. 37 (1998) 6731;
(c) T. Moriuchi, T. Nagai, T. Hirao, Org. Lett. 7 (2005) 5265;
(d) T. Moriuchi, A. Nomoto, K. Yoshida, T. Hirao, Organomettalics 20 (2001) 1008;
(e) S. Chowdhury, D.A.R. Sanders, G. Schatte, H.-B. Kraatz, Angew. Chem., Int. Ed. 45 (2006) 751;
(f) T. Moriuchi, A. Nomoto, K. Yoshida, A. Ogawa, T. Hirao, J. Am. Chem. Soc. 123 (2001) 68;
(g) I.B. Amoa, R. Silerova, H.-B. Kraatz, Chem. Commun. (2002) 2430;
(h) L. Barisic, M. Dropucic, V. Rapic, H. Pritzkow, S.I. Kirin, N. Metzler-Nolte, Chem. Commun. (2004) 2004;
(i) A. Nomoto, T. Moriuchi, S. Yamazaki, A. Ogawa, T. Hirao, Chem. Commun. (1998) 1963;
(j) L. Barisic, M. Cakic, K.A. Mahmoud, Y.-nian Liu, H.-B. Kraatz, H. Pritzkow, S.I. Kirin, N. Metzler-Nolte, V. Rapic, Chem. Eur. J. 12 (2006) 4965;
(k) T. Moriuchi, K. Yoshida, T. Hirao, Organomettalics 20 (2001) 3101;
(l) K. Heinze, M. Schlenker, Eur. J. Inorg. Chem (2004) 2974;
(m) D.A. Leigh, A. Venturini, A.J. Wilson, J.K.Y. Wong, F. Zerbetto, Chem. Eur. J. 10 (2004) 4960–4969.
[13] L. Lin, A. Berces, H.-B. Kraatz, J. Organomet. Chem. 556 (1998) 11.
[14] J.D. Carr, S.J. Coles, M.B. Hursthouse, M.E. Light, J.H.R. Tucker, J. Westwood, J. Angew. Chem., Int. Ed. 39 (2000) 3296.
[15] J. Tao, Z.-J. Ma, R.-B. Huang, L.-S. Zheng, Inorg. Chem. 43 (2004) 6133.
[16] (a) L. Cuesta, D.C. Gerbino, E. Hevia, D. Morales, M.E.N. Clemente, J. Pérez, L. Riera, V. Riera, D. Miguel, I.-d. Río, S. García-Granda, Chem. Eur. J. 10 (2004) 1765;
(b) D.H. Gibson, M.S. Mashuta, X. Yin, Acta Crystallogr., Sect. E59 (2003) m911;
(c) W. Wang, Y.K. Yan, T.S. Andy Hor, J.J. Vittal, J.R. Wheaton, I.H. Hall, Polyhedron 21 (2002) (1991).
[17] P.J. Heard, P. Sroisuwan, D.A. Tocher, Polyhedron 22 (2003) 1321.
[18] (a) G. Bandoli, A. Dolmella, Coord. Chem. Rev. 209 (2000) 161;
(b) G. Dong, L. Yu-ting, D. Chun-ying, M. Hong, M. Qing-jin, Inorg. Chem. 42 (2003) 2519.
[19] A. Togni, T. Hayashi (Eds.), Ferrocenes: Homogeneous Catalysis, Organic Synthesis, Material Science, VCH, Weinheim, Germany, 1995 (Chapter 6).
[20] D.G.L. Holt, L.F. Larkworthy, D.C. Povey, G.W. Smith, G.J. Leigh, Inorg. Chim. Acta 169 (1990) 201.
[21] H. Miyaji, S.R. Collinson, I. Prokeŝ, J.H.R. Tucker, Chem. Commun. (2003) 64.
[22] W. Knobloch, W.H. Rauscher, J. Polym. Sci. 54 (1961) 651.
[23] D.K.J. Gorecki, E.M. Hawes, J. Med. Chem. 20 (1977) 838.